

Modeling the Dynamic Behavior of Diblock Copolymer/Particle Composites

Valeriy V. Ginzburg, Corey Gibbons, Feng Qiu, Gongwen Peng, and Anna C. Balazs*

Department of Chemical and Petroleum Engineering, University of Pittsburgh, Pittsburgh, Pennsylvania 15261

Received July 1, 1999; Revised Manuscript Received May 23, 2000

ABSTRACT: We develop a coarse-grained model to investigate the influence of nanoscale particles on the phase separation and the morphology of symmetric AB diblock copolymer films. The microphase separation is modeled by the cell dynamical systems (CDS) equations, while the particle dynamics is described by the Langevin equation. We assume that the particles have a selective interaction with the A block, and we vary the interaction strength, the particle number density, and mobility. The mobile particles destroy the bicontinuous structure that is typical for symmetric diblocks. In the limit of weak interactions between the A blocks and particles, the A's form the continuous phase and the B's form isolated domains. In the case of strong particle/A block interactions, the B phase is continuous and the A blocks self-assemble into distinct islands. Thus, the character of the continuous phase can be tailored by varying the strength of the block–particle interaction.

I. Introduction

Polymer films that contain well-defined patterns form a key component in a variety of novel applications. For example, patterned polymer substrates could be used as templates in fabricating nanoscale electronic devices through the selective adsorption of a conducting material. One means of forming laterally heterogeneous or patterned polymer layers is to spin-cast a solution of AB diblock copolymers onto a substrate.¹ When the film is annealed, symmetric diblocks can microsegregate into lamellar layers that lie perpendicular to the substrate, thereby presenting a striped pattern at the free surface. While the size of these patterns depends on the block lengths,^{2–5} domains that are on the order of tens of nanometers can be readily produced. This size scale is an order of magnitude smaller than that typically achieved through photolithography. If the A and B blocks are chosen so that a metallic compound preferentially wets one of the stripes, metal can be deposited onto the polymer substrate in a highly controlled manner.^{6–8} This system of alternating polymeric and metallic nanoscopic domains should exhibit unique electrical or optical properties.

Recently, Morkved et al.^{6,8} used this prescription to fabricate films consisting of gold nanoparticles on symmetric polystyrene–poly(methyl methacrylate) (PS–PMMA) and asymmetric polystyrene–poly(2-vinylpyridine) (PS–PVP) diblock copolymers. The gold particles self-assembled into islands within the PMMA lamellae in the first case and within the PVP spherical domains in the second case. Thus, the films appear as if one of the blocks were “decorated” by the metal particles. The driving force for this type of self-assembly is a selective interaction between the particles and one of the polymeric components.

Of particular interest is determining whether and how the particles affect the structure of the underlying polymeric pattern. So far, there have been few theoretical studies of the dynamic behavior of copolymer/particle mixtures. In their recent work, Sevink et al.⁹ simulated microphase ordering in diblock copolymers with *im-*

mobile filler particles using the dynamic density functional model. They showed that the lamellar structure in the vicinity of the fillers was modified by the presence of the particles. The calculated patterns for the two-dimensional case bear some resemblance to the simulation of stationary particles in phase-separating polymer blends by Lee et al.¹⁰ While these studies improved our understanding of the influence of *individual* particles on the phase separation in blends or microphase separation in copolymers, they did not take into account the dependence of the morphology of the composite on the volume fraction or mobility of the fillers.

In this paper, we develop a numerical formalism and perform computer simulations to relate the size and the structure of the polymer domains to the concentration of solid *mobile* particles. For the computational study, we adapt our coarse-grained model (originally developed to describe the behavior of hard particles in a phase-separating binary mixture^{11,12}) to a system of solids in a film of microphase-separating diblocks. To model the selective interaction between the particles and one of the blocks (e.g., the A block), we “coat” the surface of the particles with a layer of A. In this manner, the particles preferentially localize in the A domains, and we capture essential interactions in the relevant experimental systems.^{6,8} The model also allows us to vary the particle mobility and the particle–polymer interactions, which are important in determining the morphology of the mixture.

II. Model

We represent the polymer film by a two-dimensional square lattice, which is 256×256 sites in size and has periodic boundary conditions in both the *x* and *y* directions. On each lattice site, we define the scalar order parameter $\Psi = \rho_A - \rho_B$, where ρ_A and ρ_B are the respective local densities of the A and B components. Note that $\Psi = 1$ (–1) corresponds to the equilibrium order parameter for the A-rich (B-rich) phase. Into this system, we introduce spherical particles of radius $R_0 = 1$. The particles have an affinity for the A block. This

affinity is introduced via the boundary conditions on the surface of each particle and a polymer–particle coupling term in the free energy (as described below). Thus, the particles can influence the morphology and size of the polymer domains that are formed during the microphase separation, and the polymer can affect the spatial distribution of the particles. Below, we describe the equations of motion for both the polymeric and the particulate components.

The dynamics of microphase separation in a melt of diblocks can be described through the following equation:^{2,5,14}

$$\frac{\partial \Psi}{\partial t} = M \nabla^2 \frac{\delta \mathcal{F}}{\delta \Psi} - \Gamma(\Psi - F) + \xi \quad (1)$$

The constant M is the mobility for the order parameter field. The variable $F = 2f - 1$ describes the asymmetry of the diblock; for a symmetric diblock, $f = 0.5$ and $F = 0$. The ξ term is the noise field (which we set to zero in this study), and the parameter Γ determines the thickness of the lamellar domains and is proportional to N^2 , where N is the length of the block copolymer.^{2,5}

The free energy \mathcal{F} is given by

$$\mathcal{F} = \mathcal{F}_1 + \mathcal{F}_{\text{cpl}} \quad (2)$$

Here, the local free energy term \mathcal{F}_1 is given by

$$\mathcal{F}_1 = \int d\mathbf{r} \left[f_1(\Psi(\mathbf{r})) + \frac{D}{2} (\nabla \Psi)^2 \right] \quad (3)$$

where the double-well potential f_1 is selected to be

$$f_1 = -A \log(\cosh(\Psi)) + \frac{1}{2} \Psi^2 \quad (4)$$

The coupling term \mathcal{F}_{cpl} describes the interactions between the particles and the polymer. To model this term, we select the following expression:

$$\mathcal{F}_{\text{cpl}} = C \int d\mathbf{r} \sum_i V(\mathbf{r} - \mathbf{R}_i) (\Psi(\mathbf{r}) - \Psi_s)^2 \quad (5)$$

The potential $V(\mathbf{r})$ is assumed to be exponential (although any other rapidly decaying function could also be used)

$$V(\mathbf{r}) = \exp\left(-\frac{r}{r_0}\right) \quad (6)$$

We set the “coupling range” $r_0 = 3$, so the interaction is short-ranged. (It only affects the nearest- and next-nearest-neighbor sites for a given particle.)

The motion of the particles is described by the Langevin equation,

$$\dot{\mathbf{R}}_i = M_p \left(\mathbf{f}_i - \frac{\partial \mathcal{F}}{\partial \mathbf{R}_i} \right) + \eta_i \quad (7)$$

where M_p is the particle mobility, \mathbf{f}_i is the force acting on the i th particle due to all the other particles, and η represents a Gaussian white noise with $\langle \eta_{i\alpha}(\mathbf{r}, t) \eta_{j\beta}(\mathbf{r}', t') \rangle = G_2 \delta(\mathbf{r} - \mathbf{r}') \delta(t - t') \delta_{ij} \delta_{\alpha\beta}$. In this study, we neglect interactions between particles (i.e., $\mathbf{f}_i = 0$) and consider only the particles’ diffusive motion and their interaction with the polymer.

A cell dynamical systems (CDS) method¹⁵ is used to update the value of Ψ for the phase-separating AB

mixture. By employing CDS modeling (rather than a conventional discretization of eq 1), we can significantly increase the computational speed of the simulation.¹¹

To simulate the particle dynamics, we discretize eq 7 and only allow the particles to move between different lattice sites. A “Kawasaki exchange” mechanism is used for each particle move. First, the order parameter values from all the cells to be occupied by a particle in its “new” position are moved to the “old” position. Next, the boundary and excluded-volume conditions are imposed for the order parameter at the “new” particle position. This mechanism ensures the conservation of the order parameter. Such dynamics may break down for high particle mobilities, so we considered only the case where the diffusion constant is rather low. (Almost all particle “jumps” are to neighboring sites.) The discretized equations of motion have the following form:

$$\Psi(\mathbf{r}, t+1) = F[\Psi(\mathbf{r}, t)] - \langle \langle F[\Psi(\mathbf{r}, t)] - \Psi(\mathbf{r}, t) \rangle \rangle + \xi(\mathbf{r}, t)$$

$$F[\Psi(\mathbf{r}, t)] = f(\Psi(\mathbf{r}, t)) + \frac{\delta \mathcal{F}_{\text{cpl}}}{\delta \Psi} + D(\langle \langle \Psi(\mathbf{r}, t) \rangle \rangle - \Psi(\mathbf{r}, t))$$

$$f(\Psi) = A \tanh(\Psi)$$

$$\mathbf{R}_i(t+1) = \mathbf{R}_i(t) + M_p \left(\mathbf{f}_i - \frac{\partial \mathcal{F}}{\partial \mathbf{R}_i} \right) + \eta_i(t) \quad (8)$$

where $\langle \langle \dots \rangle \rangle$ is the isotropic spatial average over the nearest-neighbor and the next-nearest-neighbor sites, and $[\langle \langle \dots \rangle \rangle - \dots]$ can be thought of as a discrete generalization of the Laplacian.

At the surface of each particle, the lattice boundary conditions (specified order-parameter value and zero order-parameter flux) are imposed as $\Psi(\mathbf{r}, t) = \Psi_s$ and $\partial_n F(\mathbf{r}, t) = 0$, if $R_0 < |\mathbf{r} - \mathbf{R}_i(t)| \leq R_0 + a$, where a is the lattice spacing and ∂_n denotes the “lattice” normal derivative. Here, we set $\Psi_s = 1$ so that the particles are “coated” by fluid A. The $\partial_n F = 0$ condition ensures zero flux of Ψ into the particles since F plays the role of a chemical potential.

We perform simulations for several systems, varying the number of particles from 0 to 400. (This corresponds to a variation of the particle volume fraction ϕ_p between 0 and 0.128.) Each system was averaged over three runs of 50 000 time steps each. For all systems, the following values of the parameters were used: $A = 1.3$, $D = 0.5$, $G_1 = 0$, $G_2 = 0.5$.¹⁶ The initial fluctuations of Ψ are Gaussian with a variance of 0.05. For all runs, the composition of the copolymer is fixed at 50:50 (symmetric diblock).

To study the role of the coupling interactions, we consider two cases: (a) $C = 0$ (no coupling) and (b) $C = 0.1$ (strong coupling). We note that low values of C ($\ll 0.1$) show very similar behavior to the $C = 0$ example. Thus, the conclusions we draw for the $C = 0$ case also apply to examples involving small C . The parameter C controls the strength of the wetting interaction between the particles and the fluids. In other words, C provides a thermodynamic driving force for the particles to be localized in the more favored phase. That the nature of coating, and thus the wetting interaction, can be exploited to control the location of the particles was recently demonstrated by Hashimoto et al.¹⁷ In particular, the researchers showed that the particles’ position and morphology of a particle/diblock film could be tailored by altering the type of the chains that are anchored to the nanoparticles.¹⁸ Another way to ef-

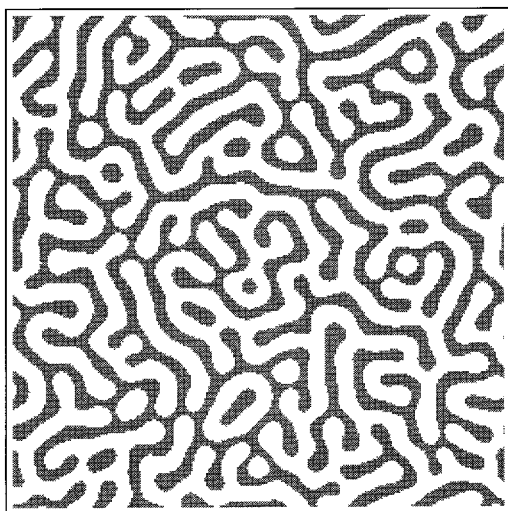


Figure 1. Late-stage ($t = 30\,000$ time steps) morphology of the symmetric diblock copolymer. Here, dark regions represent B-rich lamellae, and white regions represent A-rich lamellae.

fectively alter C , and thus affect the partitioning of the particles, is to vary the chemical nature of the particles (i.e., from gold to silver or tin).¹⁹ In our model, we capture the physical effect of varying the chemical identity of the particle or the character of the coating by varying C .

The simulation results for both cases of weak and strong coupling and the subsequent analysis are presented in the next section.

III. Results and Discussion

We first study the weak coupling case. As we noted above, the behavior for small C ($\ll 0.1$) is very similar to the case of $C = 0$. Thus, we focus on the $C = 0$ example. For such systems, the motion of particles is purely diffusive because the forces exerted by the fluids on the solids are neglected (i.e., $f_{\text{cpl}} = 0$). Because of the A “coating” on the surface of each particle, the particles “attract” A domains and “repel” B, so the majority of particles at any given time can be found in the A regions. For a binary AB mixture undergoing spinodal decomposition, the diffusing particles often break up (or “cut”) the B domains and significantly modify the morphology of the system.^{11,12} In addition, the motion of the particles slows down (possibly even stops) the coarsening process at the late stage.^{11–13}

For the diblock copolymers, the effect is complicated by the fact that the A and B domains are not independent, and the system undergoes microphase separation rather than spinodal decomposition. (The typical late-stage morphology for a symmetric diblock copolymer system is shown in Figure 1.) Nevertheless, the qualitative influence of the moving particles on the morphology is very similar to the case of binary mixtures. In Figure 2, we show the structure of the system with $N = 300$ particles ($\phi_p = 0.096$) in the early (Figure 2a), intermediate (Figure 2b), and late (Figure 2c) stages of the microphase separation. At all times, most of the particles are located in the A-rich domains, although some of them have “jumped” into B-rich areas. To lower the free energy of the system, A domains eventually engulf the A-coated particles within B. This process has the effect of “cutting” the B-rich areas into separate regions. Through this mechanism, the particles destroy the bicontinuous structure that is typical of symmetric

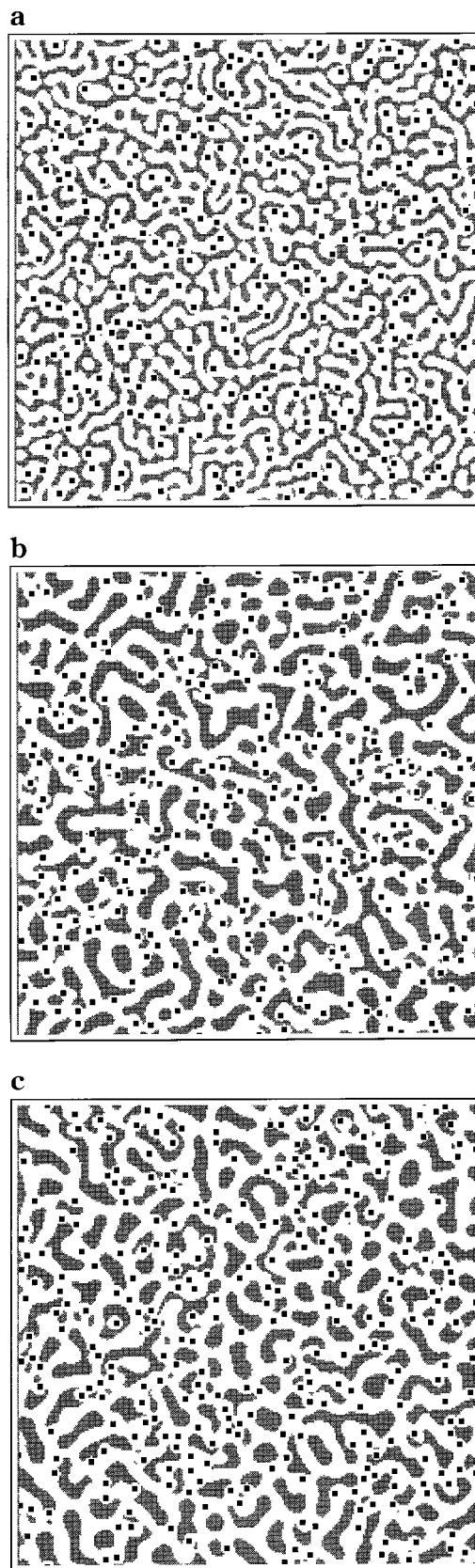


Figure 2. Morphology of the symmetric diblock copolymer with mobile particles for the “no-coupling” case ($C = 0$). The particle number density $\phi_p = 0.096$ ($N = 300$). The figures correspond to the (a) early ($t = 300$ time steps), (b) intermediate ($t = 3000$ time steps), and (c) late ($t = 30\,000$ time steps) phases of the microphase separation.

diblock systems. Now isolated regions of B are dispersed in a “sea” of A. (It would be more accurate to say that

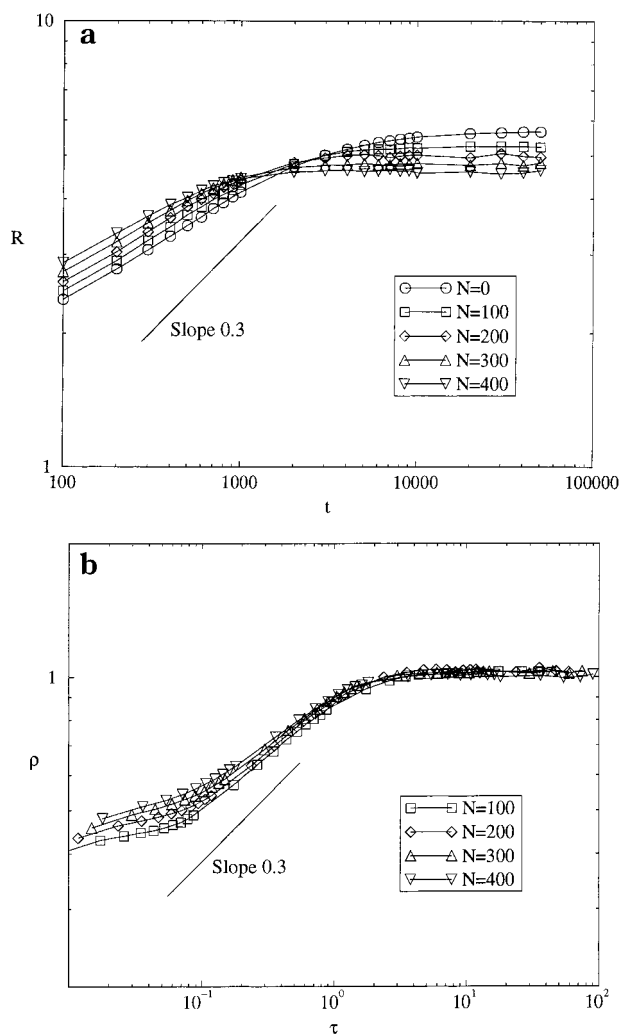


Figure 3. Characteristic lamellar size vs time for the “no-coupling” case: (a) unscaled and (b) scaled plots. The scaled domain size and the scaled time are given by $\rho = [R/(1 + \beta\phi_p)] \cdot (R_0^{-3} + \alpha\beta\phi_p)^{1/3}$ and $\tau = At(R_0^{-3} + \alpha\beta\phi_p)$. The best fit shown here corresponds to $\alpha = 0.062$ and $\beta = 1.5$.

the motion of the particles causes rearrangements of polymer chains, leading to the breakup of the B lamellae without breaking the A lamellae. The coarse-grained technique used here, however, does not allow us to probe molecular motions.)

To quantify the role of particles in determining the morphology of the mixture, we calculate the effective domain size $R(t)$ (which is synonymous with the lamellar period Δ). To calculate $R(t)$, we use the “broken bond” formula,²⁰ $R \sim L^d/A(t)$, where L^d is the volume of the system and $A(t)$ is the total interfacial “area”. For $d = 2$ this becomes

$$R = \frac{L^2}{N_x + N_y} \quad (9)$$

where L is the system size and N_x and N_y are the numbers of “broken bonds” (pairs of nearest neighbors with opposite signs of Ψ in the x and y directions, respectively). The time dependence of R for several particle densities is plotted in Figure 3a. It can be seen that, as in the case of binary mixtures,^{11,12} particles in block copolymers decrease the effective domain size. This can be attributed to the “cutting” effect and the creation of new interfaces, as discussed above.

To describe the evolution of the lamellar domains analytically, we propose the following scaling expression (which is similar in form to the expression for binary mixtures with particles^{11,12}):

$$R(t) = (1 + \Phi)(\gamma + \alpha\Phi)^{-1/3} G(At(\gamma + \alpha\Phi)) \quad (10)$$

Here Φ is the “effective particle volume fraction”, and $\gamma = (D_0)^{-3}$ where $D_0 \approx 5.62$ is the domain size of the pure diblock in the absence of particles. The variable A is a dimensionality constant (here we set $A = 0.1$ so that the crossover between the intermediate and late stages occurs at the “scaled time” of 1) and α is an adjustable parameter. The universal scaling function $G(x)$ has the following asymptotic form, $G(x) \sim x^{1/3}$ if $x \ll 1$ (the Lifshitz–Slyozov regime²¹) and $G(x) \approx 1$ if $x \gg 1$ (the late-stage regime where the domain size has saturated).

Note that we use the “effective” particle volume fraction $\Phi = \beta\phi_p$, where β is another adjustable parameter. The need for this modification stems from the fact that the particles strongly influence the surrounding fluid (via the boundary conditions) and thus require $\beta \geq 1$. This will be seen even more distinctly for the case of strong coupling.

The specific form of the scaling expression can be rationalized through the following arguments. First, because of the particles’ affinity for the A blocks, the system is effectively asymmetric, and this asymmetry is reflected in the prefactor $(1 + \Phi)$. (Such arguments are also made in the equilibrium scaling model developed by Hamdoun et al.⁷) Second, because of the mobility of the particles, the lamellar ordering is disturbed. For large particle densities and mobilities, the system can be in a metastable “steady state”, as described in ref 12 for the case of a binary blend with mobile particles. For that system, the late-stage characteristic size, $R^*(\Phi)$, was shown to scale as $\Phi^{-1/3}$. In the case of the copolymers, the system has its own length scale D_0 , the lamellar period of the pure diblocks. It is natural to assume that the final domain size is determined by the interplay between these two lengths, $R^*(\Phi)$ and D_0 . Thus, we write the second factor in the rhs of eq 10 in the form $(\gamma + \alpha\Phi)^{-1/3}$, where $\gamma = (D_0)^{-3}$. The parameter α is related to the effective mobility of the particles.¹² Finally, the choice of “scaled time” $r = At(\gamma + \alpha\Phi)$ is dictated by the requirement that at the intermediate stage the domain growth, $R(t)$, is described by the Lifshitz–Slyozov “1/3 law” and is independent of the particle number density (apart from the prefactor $1 + \Phi$).

The use of scaling expression of eq 10 allows us not only to fit all the data onto one master curve (Figure 3b) for the intermediate and late stages of the microphase separation, but it also enables one to qualitatively understand the contributions of the different processes. For the “no-coupling” case, the best fit corresponds to $\alpha = 0.062$ and $\beta = 1.5$. We see that the final domain size is determined mostly by the particle number density and mobility, since $\alpha\Phi > \gamma$ for all four systems.

We now turn our attention to the case of strong coupling ($C = 0.1$). By strong coupling, we mean that the magnitude of the coupling term is large relative to the noise term in eq 7. Here, once the system segregates into A-rich and B-rich regions, the particles essentially become “bound” to the A-rich areas. Instead of effectively intermixing the two components, the particles self-assemble into the A lamellae, swell these regions,

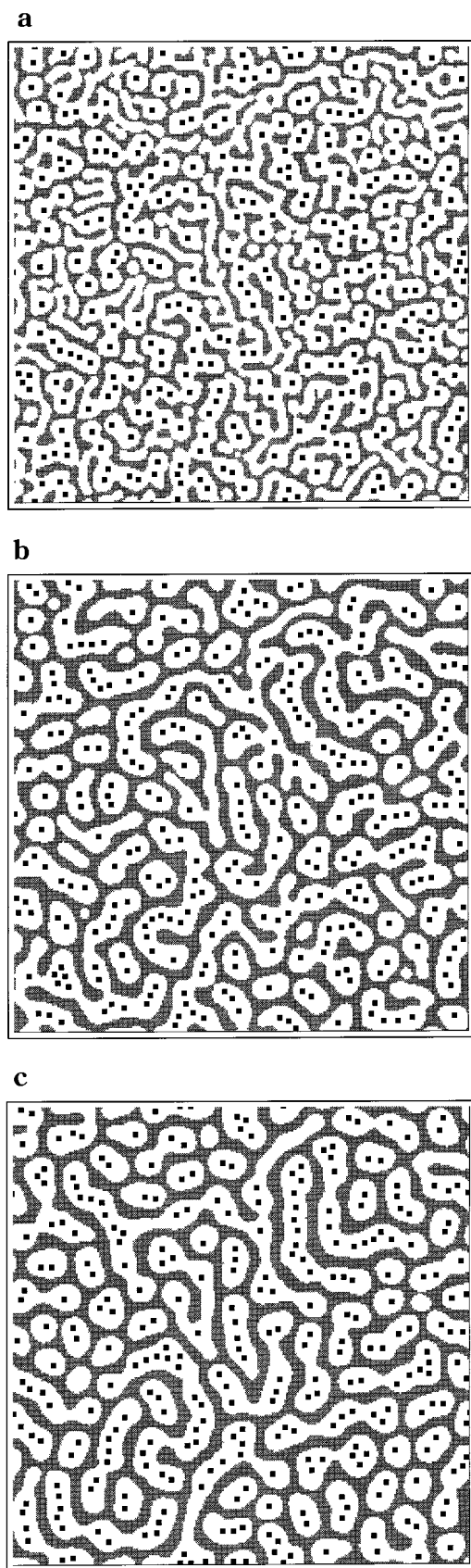


Figure 4. Same as Figure 2, but for the “strong-coupling” case ($C = 0.1$).

and thereby modify the structure of the system. We present three snapshots of this system in Figure 4 for the early (Figure 4a), intermediate (Figure 4b), and late (Figure 4c) stages of the microphase separation. As can

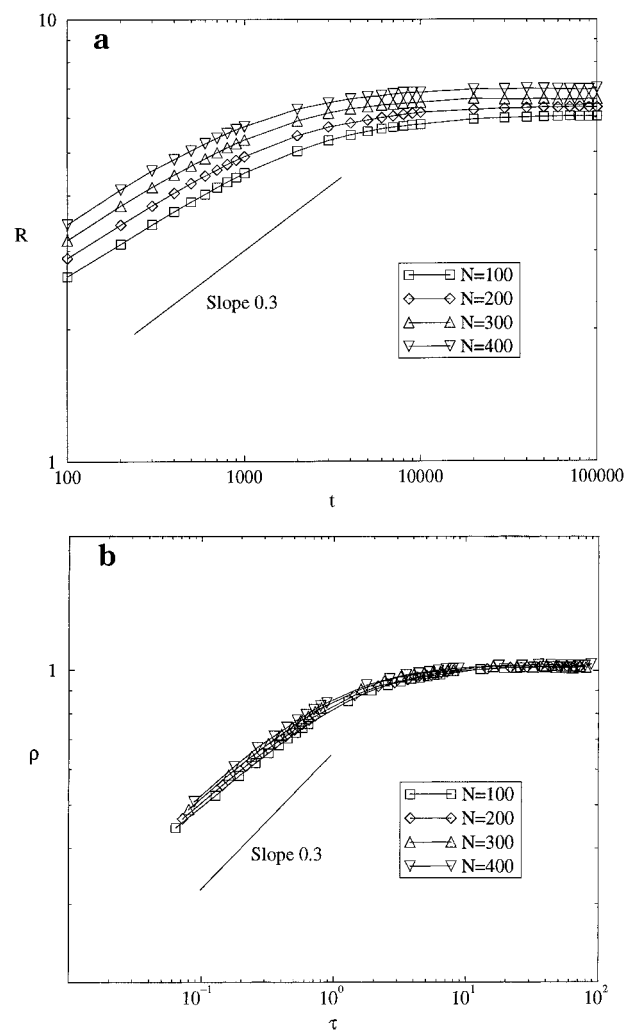


Figure 5. Same as Figure 3, but for the “strong-coupling” case ($C = 0.1$). For the scaled plot, $\alpha = 0.008$ and $\beta = 3.0$.

be seen in Figure 4c, the A's now form isolated domains and the B forms the continuous phase. Since the A domains are strongly “attracted” to and localized by the compatible particles, there is not enough of the A to form the bicontinuous structure. Note that in a mixture containing $N = 300$ ($\phi_p = 0.096$) A-coated particles, the effective composition shifts from 50:50 to approximately 60:40, with B being the minority phase. What is striking in Figure 4c is the fact that it is the minority phase that percolates.

This structure for $C = 0.1$ (Figure 4) is in sharp contrast to the morphology for $C = 0$ (Figure 2), where the A is the continuous phase and the B's form the isolated domains. Figure 4c is also different from the no-particle ($N = 0$) case, where the diblocks have self-assembled into a bicontinuous structure (Figure 1).

The structures of Figure 4b,c are qualitatively similar to the TEM micrographs obtained by Morkved et al.⁶ In the latter experiments, small (6 nm in diameter) gold particles were introduced in a film of a symmetric PS/PVMA diblock copolymer. Because of the affinity of the gold for PS block, all the particles self-assembled in the PS-rich lamellae, forming “islands” similar to those shown in Figure 4.

The time dependence of the domain size R for the strong-coupling case is shown in Figure 5a. In the case of strong coupling, the particles have the opposite effect on the domain size than in the “no-coupling” case; as

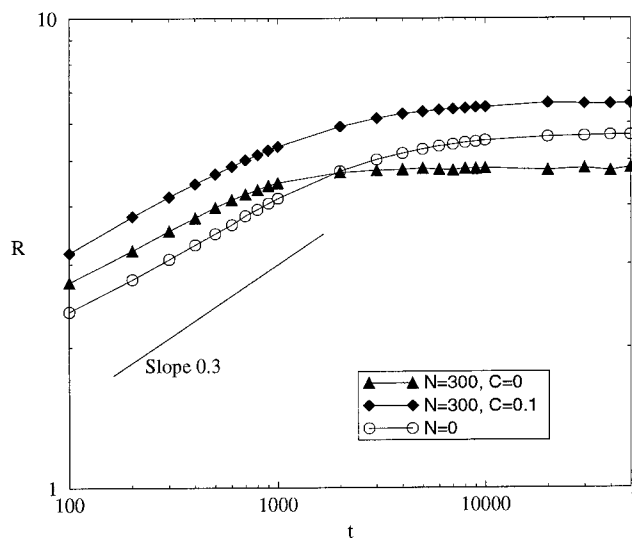


Figure 6. Characteristic lamellar size vs time for the $\phi_p = 0.096$ ($N = 300$) system with ($C = 0.1$, filled diamonds) and without ($C = 0$, filled triangles) coupling interaction. The lamellar size for the no-particle system (open circles) is also plotted for comparison.

the particle number density is increased, the lamellar period also increases. This is easily understood since the particles now swell the A lamellae instead of breaking up the B lamellae. We can again use our scaling formula to collapse all the data onto one master curve (Figure 5b). The best fit now corresponds to $\alpha = 0.008$ and $\beta = 3.0$.

To better understand the role of the coupling interaction on the dynamics of microphase separation, we plot the characteristic size vs time for the case $N = 300$ with $C = 0$ (filled triangles) and $C = 0.1$ (filled diamonds) in Figure 6. The no-particle case (open circles) is shown for the sake of comparison. It can be seen that at the early stage of microphase separation domain growth is facilitated by particles. The coupling interaction between the particles and the A block enhances this process, resulting in the increase in the domain size. At the late stage, the characteristic size is determined not only by the particle number density but also by the effective particle mobility. As noted above, strong coupling "pins" the particles inside the A domains and prevents them from creating new interfaces and destroying the lamellar ordering. Thus, the domain size is largest for the strong-coupling case and smallest for the no-coupling case.

The above analysis shows that the mobility of the particles is an important factor in determining the structure of the mixture. Indeed, when the particles are sufficiently mobile that they can "jump" over the interfaces and cause the rearrangements of the domain morphology (the no-coupling case), the overall structure becomes more disordered than in the absence of particles. When the mobility of the particles is suppressed, for example, by the strong-coupling interaction, which "anchors" the particles to one of the blocks, the particles actually enhance the ordering and create new self-assembled structures.

An interesting case is where the particles are actually immobile (being pinned to the substrate, for example). In Figure 7, we show the late-stage morphology for such a system, also with $N = 300$ and $C = 0.1$. In contrast to the mixture with mobile particles, the morphology of the system remains bicontinuous. Similar bicontinuous

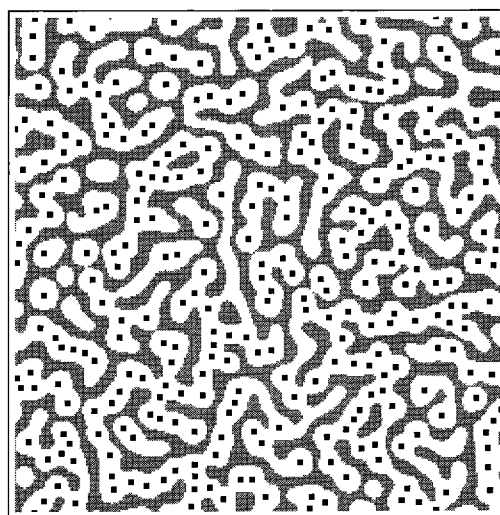


Figure 7. Late-stage ($t = 30\,000$ time steps) morphology for the system with $N = 300$ immobile particles in the "strong-coupling" ($C = 0.1$) case.

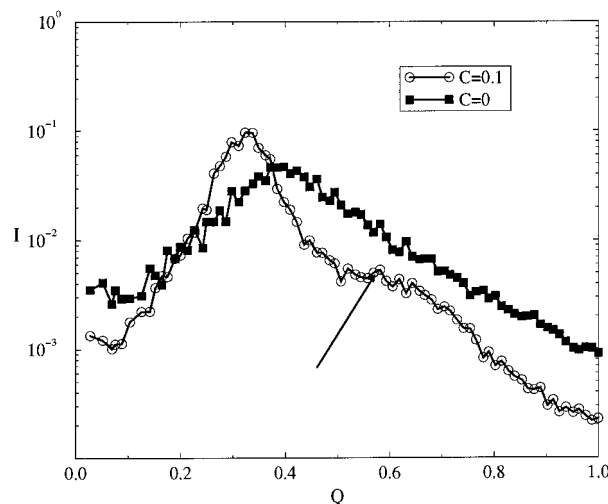


Figure 8. Scattering function (linear-log plot) of the diblock copolymer/particle system at $t = 30\,000$ for the "strong-coupling" ($C = 0.1$, open circles) and "no-coupling" ($C = 0$, filled squares) cases. The arrow indicates the high- Q shoulder for the "strong-coupling" case.

structures are also seen for immobile particles with $C = 0$.

We also examined the influence of coupling on the structure and dynamics of the interfaces in the system. In Figure 8, we plot the circularly averaged scattering factor $I(Q, t)$ defined by

$$I(Q, t) = \frac{1}{2\pi} \int_0^{2\pi} d\theta \int d\mathbf{r} \langle \Psi(\mathbf{r}, t) \Psi(\mathbf{0}, t) \rangle \exp(i\mathbf{Q} \cdot \mathbf{r}) \quad (11)$$

where θ is the angle between \mathbf{Q} and the arbitrarily chosen base direction. To ensure the smooth behavior of the scattering function, we substitute $\Psi = \Psi_s$ everywhere within the particles. The scattering function $I(Q, t)$ is calculated for the system with $N = 300$ particles at the time $t = 30\,000$ time steps; the results are averaged over three independent runs. The filled squares correspond to the no-coupling ($C = 0$) case; the open circles depict the strong-coupling ($C = 0.1$) case. It can be seen that the coupling not only shifts the position of the main peak toward lower Q but also forms a "shoulder" in the high- Q region (indicated by an arrow).

It is argued²² that such a shoulder is related to the "roughness" of the interfaces; when the lamellar interfaces are well-defined and smooth, the scattering function acquires a small peak near $2Q_{\max}$, where Q_{\max} is the location of the main peak. In the absence of coupling, the particles constantly "cut" the interfaces, and there is no shoulder in the scattering function in the large- Q region. Thus, the scattering function effectively confirms our conclusions from the visual inspection of morphologies shown in Figures 2 and 4.

IV. Conclusions

We developed a model to simulate the microphase separation in diblock copolymer/particle mixtures. The model combines a coarse-grained description of the microphase separation for the copolymer with the Langevin dynamics for the particles. The particles have an affinity for one of the polymers (block A) and thus can influence the lamellar ordering of the copolymer. The structure of the mixture will depend on the particle number density, mobility, size, the strength of the particle-polymer interaction, and the copolymer composition. In this study, we considered only symmetric diblocks and varied the number density of particles and the strength of the particle-polymer interaction ("coupling"). The cases of "no coupling" ($C = 0$) and "strong coupling" ($C = 0.1$) were studied in detail. For each case, we investigated the dependence of the morphology and the domain size on the particle number density.

In the "no-coupling" case, where the particles move purely diffusively, the lamellar structure of the diblock is effectively destroyed at even moderate particle densities ($\phi_p \approx 0.1$). Indeed, any time a particle jumps from an A-rich region to a B-rich region, it creates new interfaces and rearranges the lamellar structure. Above a certain particle density, the interfaces cannot "heal" because the jumps occur frequently. Thus, the morphology changes from the typical lamellar structure (Figure 1) to one with disconnected islands of B dispersed in a sea of A (Figure 2c). The picture changes, however, when the interaction between the particles and the A block is increased (Figure 4). The coupling force prevents particles from moving out of A domains, so no new interfaces are formed. At moderate particle densities ($\phi_p \approx 0.1$), the particles self-assemble into isolated A islands (Figure 4b,c), in qualitative agreement with recent experiments by Morkved et al.⁶ The importance of the coupling interactions can also be seen from the scattering function (Figure 8), where the small peak (or "shoulder") corresponding to the interfaces is seen for the "strong-coupling" case but disappears for the "no-coupling" case.

We also examined the role of particle mobility. When the particles are immobile, the lamellar structure and period are approximately the same as in the no-particle case; the particles only introduce some additional defects in the lamellar pattern. (This conclusion agrees qualitatively with the results of Sevink et al.⁹ that were obtained using the dynamical density functional method.) The particle mobility in the "strong-coupling" case allows the system to remove some of these defects due to the particle self-assembly. On the other hand, the particle mobility in the "no-coupling" case increases the number of such defects and eventually destroys the lamellar ordering altogether.

On the basis of these studies, we can conclude that the morphology of the particle/block copolymer mixture

can be tailored by varying the strength of the selective particle/A block interaction. The strength of this interaction is governed by the effective Flory-Huggins parameter, $\chi = \chi_{PB} - \chi_{PA}$, where χ_{PB} is the Flory-Huggins parameter between particles and the B block and χ_{PA} is the Flory-Huggins parameter between the particles and the A block. (In our model, we use the strength of the coupling potential, C , in place of χ .) Our results indicate that when the wetting or coupling interaction is very weak (less than kT), the thermal motion of the particles would dominate, and the particles would destroy the lamellar ordering.¹⁸ On the other hand, when strength of the interaction is greater than kT , the "coupling" forces would dominate, and the particles would self-assemble into the finite-sized A domains. Further experimental studies are needed to verify this prediction.

We plan to expand the above model to include other factors that play an important role in the behavior of block copolymer/particle systems, such as the interaction with the substrate and viscosity differences between the two polymers. We also plan to perform the simulations in three dimensions to elucidate the role of the film height in the pattern formation. These studies are currently underway.

Acknowledgment. We thank Profs. David Jasnow, Anne Mayes, and Heinrich Jaeger for valuable discussions. A.C.B. gratefully acknowledges support from the Army Office of Research, NSF, and DOE.

References and Notes

- (1) Kellogg, G. J.; Walton, D. G.; Mayes, A. M.; Lambooy, P.; Russell, T. P.; Gallagher, P. D.; Satija, S. K. *Phys. Rev. Lett.* **1996**, *76*, 2503.
- (2) Ohta, T.; Kawasaki, K. *Macromolecules* **1986**, *19*, 2621.
- (3) Chakrabarti, A.; Toral, R.; Gunton, J. D. *Phys. Rev. Lett.* **1989**, *63*, 2661.
- (4) Oono, Y.; Shiwa, Y. *Mod. Phys. Lett. B* **1987**, *1*, 49.
- (5) Oono, Y.; Bahiana, M. *Phys. Rev. Lett.* **1988**, *61*, 1109.
- (6) Morkved, T. L.; Wiltzius, P.; Jaeger, H. M.; Grier, D. G.; Witten, T. A. *Appl. Phys. Lett.* **1994**, *64*, 422.
- (7) Hamdoun, B.; Ausserre, D.; Cabuil, V.; Joly, S. *J. Phys. II* **1996**, *6*, 493; **1996**, *6*, 503; **1996**, *6*, 1207. Lauter-Pasiuk, V.; Lauter, H. J.; Ausserre, D.; Gallot, Y.; Cabuil, V.; Hamdoun, B.; Kornilov, E. I. *Physica B* **1998**, *241-243*, 1092. In these papers, the particle size is significantly smaller than the equilibrium lamellar thickness. We consider particles with size only slightly smaller than the equilibrium lamellar thickness, as in ref 6.
- (8) Lin, B. H.; Morkved, T. L.; Meron, M.; Huang, Z. Q.; Viccaro, P. J.; Jaeger, H. M.; Williams, S. M.; Schlossman, M. L. *J. Appl. Phys.* **1999**, *85*, 3180. Zehner, R. W.; Lopes, W. A.; Morkved, T. L.; Jaeger, H.; Sita, L. R. *Langmuir* **1998**, *14*, 241.
- (9) Sevink, G. J. A.; Zvelindovsky, A. V.; van Vlimmeren, B. A. C.; Maurits, N. M.; Fraaije, J. G. E. M. *J. Chem. Phys.* **1999**, *110*, 2250.
- (10) Lee, B. P.; Douglas, J. F.; Glotzer, S. C. *Phys. Rev. E* **1999**, *60*, 5812.
- (11) Ginzburg, V. V.; Paniconi, M.; Qiu, F.; Peng, G.; Jasnow, D.; Balazs, A. C. *Phys. Rev. Lett.* **1999**, *82*, 4026.
- (12) Ginzburg, V. V.; Qiu, F.; Peng, G.; Jasnow, D.; Balazs, A. C. *Phys. Rev. E* **1999**, *60*, 4352.
- (13) Tanaka, H.; Lovinger, A. J.; Davis, D. *Phys. Rev. Lett.* **1994**, *72*, 2581.
- (14) Glotzer, S. C.; DiMarzio, E. A.; Muthukumar, M. *Phys. Rev. Lett.* **1995**, *74*, 2034.
- (15) Oono, Y.; Puri, S. *Phys. Rev. A* **1988**, *38*, 434; **1988**, *38*, 1542.
- (16) We can relate our model parameters to the characteristics of "real" experimental polymeric films by setting the units of length, 1 lattice unit = 1 nm, and time, 1 time step = 10^{-2} s. In this case, our selection of parameters for the particle and

fluid mobilities would describe a diblock copolymer with a characteristic microphase separation time of roughly 100 s and viscosity of approximately 5×10^4 Pa s. These values are in the range of those experimentally observed for high molecular weight diblock copolymers.

- (17) Tsutsumi, K.; Funaki, Y.; Hirokawa, Y.; Hashimoto, T. *Langmuir* **1999**, *15*, 5200.
- (18) In fact, at relatively high concentrations, particles coated with P2VP-*b*-PI copolymers strongly affected the microphase separation of pure P2VP-*b*-PI diblock films, preventing these copolymers from assembling into a lamellar morphology.
- (19) Jaeger, H., private communication.
- (20) Ohta, T.; Jasnow, D.; Kawasaki, K. *Phys. Rev. Lett.* **1982**, *49*, 1223.
- (21) Lifshitz, I. M.; Slyozov, V. V. *J. Phys. Chem. Solids* **1961**, *19*, 35.
- (22) Kuwahara, N.; Kubota, K. *Phys. Rev. A* **1992**, *45*, 7385. MA991065T